Journal of Biomolecular Sctructure & Dynamics
ISSN 0739-1102
Volume 16, Issue Number 3 pp 723-732 (1998)

Computer Simulation Studies of the Fully Solvated Wild-type and Mutated GnRH in Extended and β-turn Conformations

Mihaly Mezei[1] and Frank Guarnieri[1,2]

[1]Department of Physiology and Biophysics
Mount Sinai School of Medicine, CUNY,
New York, NY 10029, USA.

and

[2]Sarnoff Corporation
201 Washington Road
Princeton, NJ 08543

This article is dedicated to David Beveridge in the occasion of his 60th birthday.

Abstract.

The conformational preference of the gonadotropin-releasing hormone (GnRH) and its Lys-8 mutant, studied earlier with a continuum model, was revisited using an explicit solvent model and thermodynamic integration to calculate the solvent's contribution to the conformation-dependence of its free energy. In addition, the Proximity Criterion was used to further analyze the effects of conformational changes.

Introduction

The gonadotropin-releasing hormone (GnRH) is the essential neuroendocrine regulator in reproductive biology. This key decapeptide hormone is generated in the hypothalamus, released into the portal circulation, and binds to GnRH receptors (GnRHR) in the pituitary leading to the release of the leutenizing and follicle-stimulating hormones. The important role of GnRH in neuroendocrinology has made it the object of intense study for many decades (1). As early as 1976 Momany performed simulations indicating the preference of the GnRH to adopt a beta-type turn conformation (2). Recently, using the new computational

technique of conformational memories (3), it was demonstrated that more than 50% of the Boltzmann distribution of conformational states of the GnRH exists in a type II beta turn around residues 5-8. (4) This conformation was shown to correspond to the NMR structure of a cyclic antagonist of GnRH (5) which binds to the GNRHR with nanomolar affinity. Additionally, the low affinity Lys8-GnRH mutant, had only about a 5% population of type II beta turn from conformational memories simulations strongly implicating the eighth position as a conformational determinant of biological activity. The original study employed a continuum solvent model. In this paper, we perform explicit water simulations on the biologically relevant conformations discovered with conformational memories.

Three of the concepts used in the calculations described in this paper originated from Prof. Beveridge. In the late seventies he initiated the application of the just emerging free energy methodology to liquid water (6). Later work in his laboratory lead to the concept of 'Full Free Energy Simulation' (7). The analysis of the solvation environment described in this paper is based on the Proximity Criterion defined by Prof. Beveridge (8).

Methods

All simulations used the Metropolis algorithm (9) with the force-bias sampling technique of Pangali, Rao and Berne (10). As proposed earlier (11), the λ-factor of force-biasing was reduced near the solute. The frequency of attempted moves was increased near the solute with the Preferential Sampling technique of Owicki (12). A bitmap was used to keep track of waters in each other's vicinity (13).

The solute was held rigid during the simulation. This restriction is in the spirit of the 'Full Free Energy Simulation' concept advocated in (7) where it is suggested that the intramolecular contributions to the free energy be studied as a separate step. While advances of computer power might seem to make this separation (and the introduction of the concomittant neglect of the coupling between the two type of energies) unnecessary, the fact remains that the timescale of solvent relaxation can be easily two or three orders of magnitude slower than the relaxation of the solute. Thus, the larger the sysytem and, especially, the change studied, the more questionable is the adequacy of sampling all the incrased number of intramolecular degrees of freedom (brought about by the flexibility of the solute), in an explicit solvent simulation.

Furthermore, when the free energy difference between two conformation of the same molecule is calculated, the difference in the intramolecular contributions can be reasonably approximated by the difference in the intramolecular energies — this approximation is equivalent to the assumption that the intramolecular entropies cancel. For the alanine dipetide it was shown (14) that this approximation involves an error of the order of kT.

Free energy simulations

Calculation of the solvation free energies with explicit solvent models is a computationally arduous task. The methodologies are generally based on a path that connects the two systems in the configuration space and on some quantity whose Boltzmann average is related to the free energy. The range of options has been reviewed in several publications (7,15-18) Among

these options, thermodynamic integration (*vide infra*) on a polynomial path (a generalization of the 'nearly linear path' (19,20,21,17)) was shown to be particularly well suited to changes involving the creation of new atoms (22,23) since it leads to a very smooth path and thus it scales very well with increasing solute size. The polynomial path is defined by a coupling parameter λ and a set of exponents $\{k_{\rm e}\}$ used for the different types of potential energy terms:

$$E(\lambda) = \sum_{\rm e=12,6,1} (1-\lambda)^{\rm k_e} EI_0(e) + \lambda^{\rm k_e} EI_1(e) \tag{1}$$

where $EI_0(e)$ and $EI_1(e)$ are the terms of the energy functions involving $1/r^{\rm e}$ of the two systems between which the free energy difference is to be computed, and λ varies from 0 to 1. Thermodynamic integration (TI), based on ideas of Kirkwood (24), relates the free energy difference between two systems to the integral

$$\Delta A = A_1 - A_0 = \int_0^1 \langle \partial E(\lambda)/\partial\lambda \rangle_\lambda d\lambda. \tag{2}$$

Substituting Eq. (1) into Eq. (2) gives

$$\Delta A = \int_0^1 \sum_{\rm e=12,6,1} k_{\rm e} \left[-(1-\lambda)^{\rm k_e - 1} \langle EI_0(e) \rangle_\lambda + \lambda^{\rm k_e - 1} \langle EI_1(e) \rangle_\lambda \right] d\lambda \tag{3}$$

For transitions involving the creation and/or annihilation of atoms a potential of the form $1/r^{\rm e}$ contributes to the integrand an asymptotic behavior of $\propto \lambda^{({\rm kd/e})-1}$ where d is the dimensionality of the space (7). Thus k should be selected high enough to keep the asymptotic behavior finite (7,25,26). Clearly, in three dimensions $k \geq e/3$ insures a convergent integrand.

Analysis of the solvation environments

The Proximity Criterion, introduced by Mehrotra and Beveridge (8,27) formed the basis of the analysis of the solvation environment. This approach partitions the space occupied by the solvent into the Voronoi polyhedra (28) generated by the bisector planes between solute atom pairs, labels the solvent in each configuration with the solute atom generating that polyhedron and calculates various averages and distributions (QCDF's (29)) for each type of solvent separately.

The Proximity Criterion has also been generalized to use radical planes (30) instead of bisectors to provide a mechanism for factoring in differences among the solute atoms (31): radical planes are the loci of point from where tangents of equal length can be drawn to spheres (of possibly different sizes) centered around two points. The radical plane will be farther from the point whose sphere is larger, resulting in generally larger solvation region. The sphere radius can be the actual atomic radius or it can be related to the solute-solvent

energy solvating that atom (e.g., to the partial charge q of that atom (31)). In this work, the radical planes were based on the solute atoms' partial charge (following ref 31) by defining a pseudo sphere radius as $R = 1.5q/q_{\max}$.

The following quantities were examined:

1. $V_{\rm fs}$, the volume of the first solvation shell. This quantity is similar in nature to the often calculated solvent-accesible surface, but is generally more useful since it also includes the effect of neighbouring groups on accessibility.

2. $\langle K \rangle$, the coordination number;

3. $\langle K \rangle / V_{\rm fs}$, the density in the first shell.

4. $\langle BE \rangle$, the binding energy of all waters in the first shell;

5. $\langle BE \rangle / \langle K \rangle$, the binding energy per water in the first shell;

6. $\langle E_{\rm ww} \rangle$, the water-water energies in the vicinity of the solute. This quantity is generally a sensitive indicator of the structure making/breaking nature of the solute.

Most of these quantities depend on the definition of the first shell radius. Generally, it is taken as the distance of the first minimum in the radial distribution function. However, taking different values for the same atom in different conformation (or in different residues) may complicate the comparison of the data. In the present work the first shell radii (somewhat arbitrarily) were obtained from the 'straight' run on the wild type. The minimum of the radial distribution function of each solute atom (describing the density fluctuations in the respective proximity regions) was determined and averaged for each solute atom type.

Calculations

At the outset, one representative turn and one extended conformation was selected from the simulation histories (4) of the wild type and the mutant, respectively. These conformations are shown on Figure 1.

The simulation box was a face-centered cubic (FCC) cell with inside sphere radius of 25.51 $\mathring{A}$, containing a peptide molecule and 2981 or 2982 water molecules (for the wild type or mutant, respectively). The calculations were run at 298 K temperature. The TIP4P (32) model was used for water and the united-atom Amber force field described the solute-solvent interactions.

The program MMC was used in all calculations. This program originated in the Beveridge Laboratory and contains contributions from Prof. Beveridge and most members of his Laboratory at Hunter College: Gary Schnelle, S. Swaminathan, Mihaly Mezei, Prem Mehrotra, Peter Maye, and B. Jayaram. The name MMC was suggested by Prof. Beveridge where the two M's perform multiple duties: Metropolis, Mihaly, Mezei, Mehrotra, Monte; and the C stands for Carlo as in Monte Carlo.

The GnRH-solvent interactions used the minimum image convention while the solvent-solvent interactions were calculated with a spherical cutoff, 7.75 Å. The minimum image convention was used for the GnRH-solvent interaction to avoid possible partitioning of the simulation cell into two regions with significant energy difference and a concomittant artifactual density jump at the sphere boundary.

Thermodynamic integration over the polynomial path with the exponent set of $\{4, 3, 2\}$ was performed using 5-point Gaussian quadrature to calculate the solvent contribution to the solvation free energy difference between different solute conformations. At each quadrature point, 10 and 20 million configurations were generated for the mutant and the wild type, respectively (the wild-type run was doubled to ascertain the stability of the result).

The error estimates for the calculated free energies were derived from the error estimates on the integrands calculated at each quadrature point using the method of batch means (33,34) based on 10^5 Monte Carlo step blocks. The estimates given represent two standard deviations.

For the proximity analysis separate 20M long simulations have been performed on both conformations of both the wild type and the mutant, supplemented by an othr 20M long simulation on the corresponding pure water system (2981 waters, 0.997 g/ml, FCC periodic cell).

Table I.
GnRH turn - extended (free) energy differences

	Wild type	Mutant
ΔE(intra)	-13.4	+16.9
ΔA(solvation,MC)	+14.2±2	-19.1±2
ΔE(solvation)	-172±27	+158±26
ΔE(GnRH-solvent)	+17	-18
$\Delta A \simeq \Delta E(\text{intra}) + \Delta A(\text{solv}, \text{MC})$	+0.9±2	-2.2±2
$\Delta A(\text{solvation}, \text{CONT})$	+10.7	-5.5
$\Delta A \simeq \Delta E(\text{intra}) + \Delta A(\text{solvation}, \text{CONT})$	-2.7	+11.4

Legend: a.) E(intra) calculated by the continuum model of Ref. 35; b.) ΔA(solvation,MC) was calculated by TI using the explicit solvent model; c.) ΔE(solvation) and ΔE(GnRH-solvent) were calculated from canonical ensemble simulations; d.) All energies are in kcal/mol.

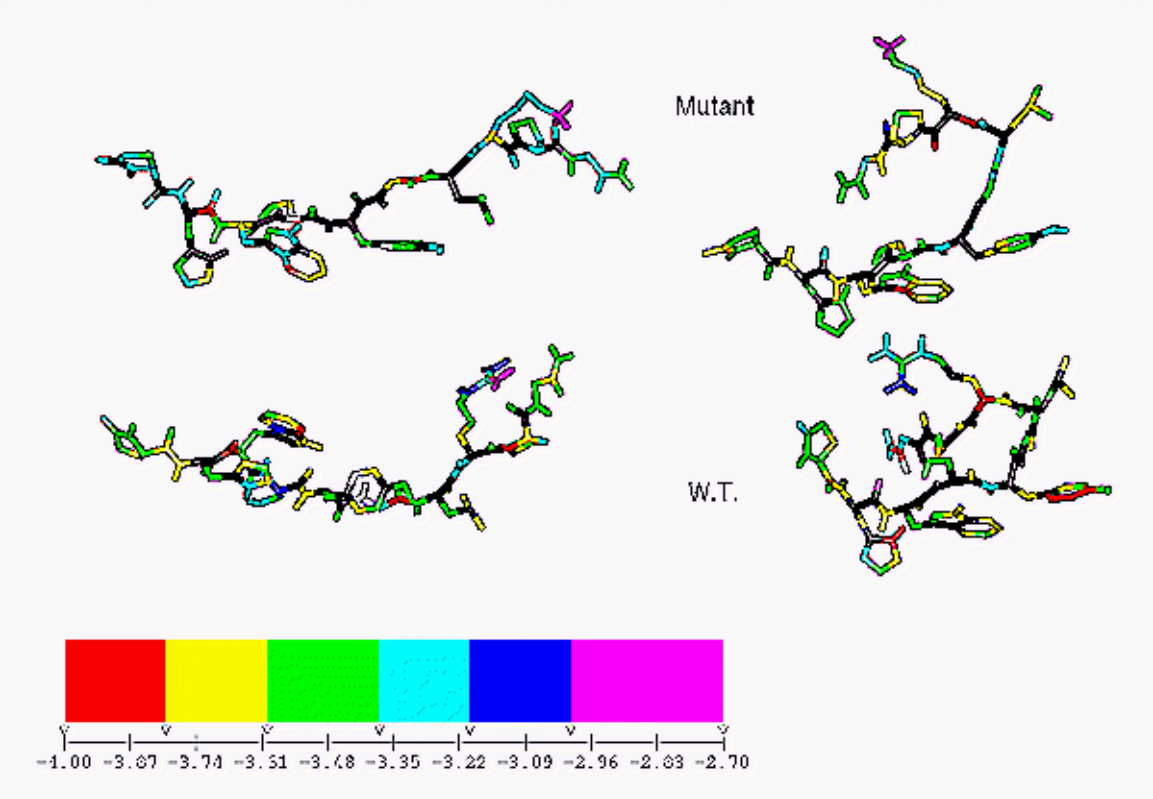

Fig. 1. Simulated GnRH conformations. Clockwise form upper left: GnRH-Lys8 (extended), GnRH (extended), GnRH-Lys8 (turn), GnRH (turn). Atoms inaccessible to the solvent are colored black. Other colors represent the solvent-solvent pair energy in the respective proximity regions. The bulk water value separates the green and cyan region

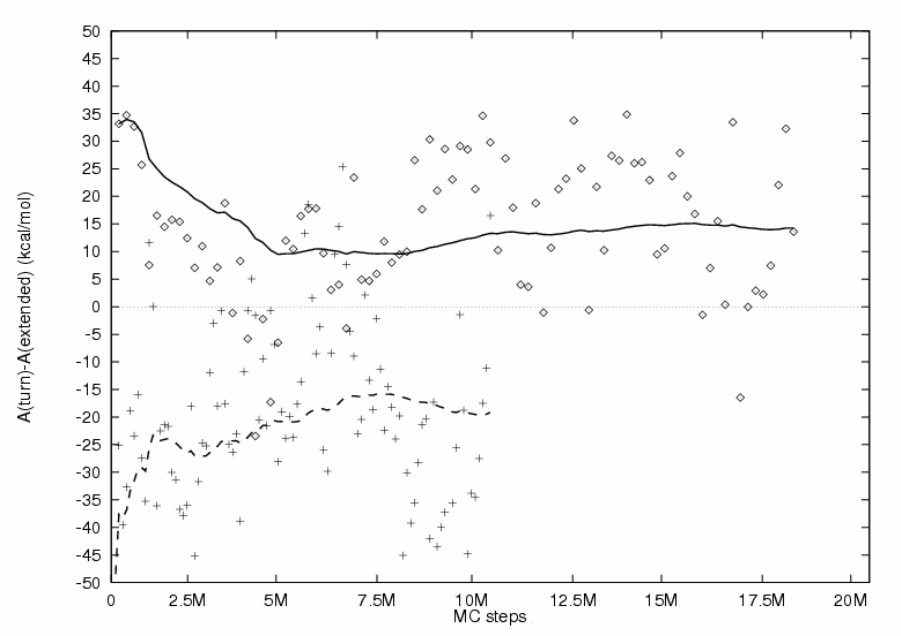

Fig. 2. Convergence profile of the calculations. 100K block averages (◊ and + for the wild-type and the mutant, respectively) and cumulative averages (full line and broken line for the wild-type and the mutant, respectively).

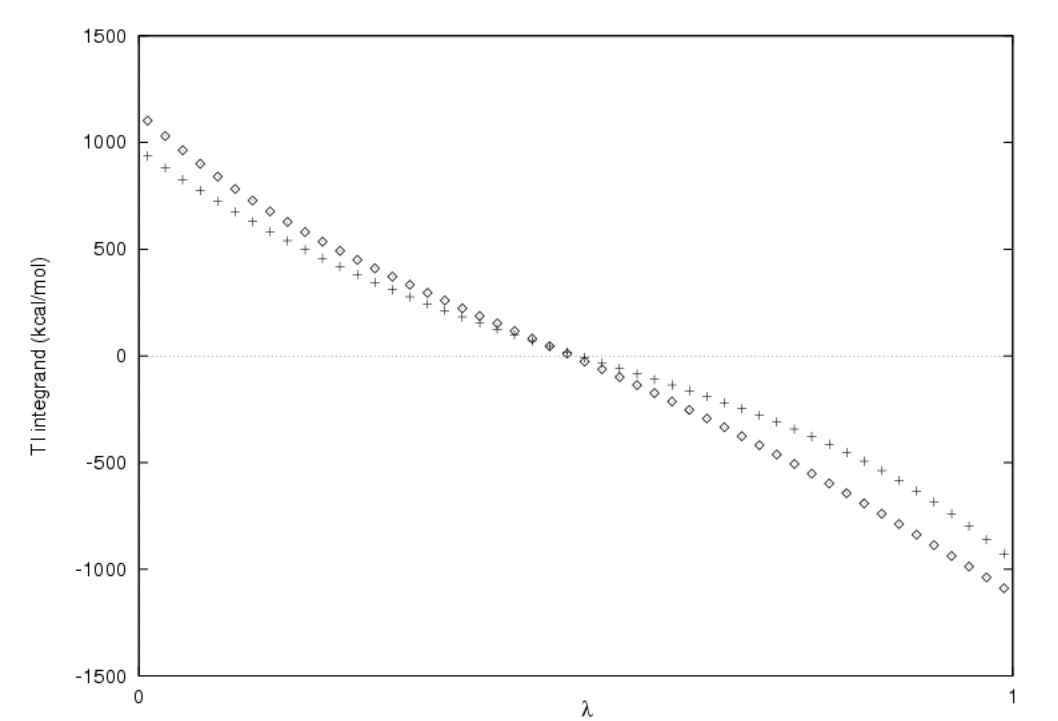

Fig. 3. The TI integrands (in kcal/mol) for the calculation on the wild-type (◊) and the mutant(+).

Results and Discussion

Table I presents the thermodynamical quantities calculated from the simulations: a.) solvation free energy differences between a fixed extended and turn conformations calculated for both the wild type and the mutant GnRH using the explicit solvents (calculated by polynomial thermodynamic integration); b.) the internal energy differences (obtained from the four canonical ensemble simulations of the two conformers of the wild type and the mutant); and c.) the differences in solute-solvent interaction energies for the wild type and the mutant. It also includes the results of single-point calculations: a.) the intramolecular energy differences for the wild type and the mutant; b.) the continuum model estimates of the free energy differences, based on the continuum solvation model of Still et al. (35); c.) the estimates of the total free energy differences as a combination of the intramolecular energy and solvation free energy differences.

The convergence profile of the free energy is shown of Figure 2. The integrand of the thermodynamic integration, shown on Figure 3, is again found to be nearly linear indicating that the quadrature error is small. This confirms our earlier conclusion (23) about the adequacy of 5-point Gaussian quadrature in conjunction with the polynomial TI.

For both conformations significant compensation was found between the intramolecular energy and the solvation free energy. This compensation reduced the estimated cost of conformational change by an order of magnitude for both molecules.

The Boltzmann distribution of conformational states obtained with the simulation technique of conformational memories indicates that the endogenous hormone GnRH preferentially populates a type II β turn structure, while the mutant hormone Lys8-GnRH preferentially populates an extended conformation. Our explicit water free energy simulations show that the extended conformation of GnRH and the type II β turn structure of Lys8-GnRH are strongly solvent stabilized. These results implicate ligand desolvation as a major determinant of recognition at the GnRHR because:

1. The type II β turn structure of the ligand binds to the receptor

2. The extended conformation of the GnRH is strongly solvated relative to the type II β turn structure

3. The type II β turn structure of the Lys8-GnRH is strongly solvated relative to the extended conformation

4. Presumably, the type II β turn structure must desolvate in order to bind at the GnRHR

5. Thus, GnRH pays a minimal desolvation penalty for GnRHR recognition, while Lys8-GnRH must pay a large desolvation penalty for binding at the GnRHR

6. Experimentally, GnRH has nanomolar affinity for the GnRHR, Lys8-GnRH has micromolar affinity for the GnRHR.

Table II

Proximity analysis results on the wild type GnRH

	Conf.	$V_{\rm fs}$	$\langle K \rangle$	$\langle K \rangle / V_{\rm fs}$	$\langle BE \rangle$	$\langle BE \rangle / \langle K \rangle$	$\langle E_{\rm ww} \rangle$
PYR	Turn	802.1	21.09	0.79	-34.32	-1.63	-3.443
HIS	Turn	501.2	10.80	0.65	-14.47	-1.34	-3.542
TRP	Turn	627.2	12.33	0.59	-14.67	-1.19	-3.644
SER	Turn	283.8	6.53	0.69	-20.05	-3.07	-3.455
TYR	Turn	844.7	21.77	0.78	-27.74	-1.27	-3.530
GLY	Turn	189.9	3.97	0.63	-13.50	-3.40	-3.605
LEU	Turn	798.9	19.17	0.72	-20.69	-1.08	-3.612
ARG	Turn	548.7	10.51	0.58	-33.79	-3.22	-3.366
PRO	Turn	431.5	10.22	0.71	-15.27	-1.49	-3.617
GLY	Turn	157.7	2.81	0.54	-5.65	-2.01	-3.685
NH2	Turn	36.6	0.10	0.09	-0.36	-3.42	-3.329
GnRH	Turn	5222.	119.30	0.69	-200.51	-1.68	-3.522
PYR	Ext.	872.1	25.67	0.89	-33.03	-1.29	-3.448
HIS	Ext.	476.1	10.18	0.64	-19.04	-1.87	-3.560
TRP	Ext.	729.7	18.36	0.76	-20.85	-1.14	-3.624
SER	Ext.	454.9	12.34	0.82	-19.08	-1.55	-3.427
TYR	Ext.	740.8	18.76	0.76	-26.56	-1.42	-3.532
GLY	Ext.	191.7	4.24	0.67	-15.14	-3.57	-3.559
LEU	Ext.	719.6	17.85	0.75	-18.66	-1.05	-3.664
ARG	Ext.	560.4	11.39	0.61	-27.55	-2.42	-3.258
PRO	Ext.	487.9	12.19	0.75	-19.32	-1.58	-3.496
GLY	Ext.	373.4	10.59	0.85	-18.82	-1.78	-3.457
NH2	Ext.	55.0	0.08	0.05	-0.25	-2.94	-3.480
GnRH	Ext.	5662.	141.68	0.75	-218.31	-1.54	-3.491

Legend: The quantities are defined in Section II.2. Energies are in kcal/mol. The first shell density is given in g/ml.

Recent work has demonstrated the importance of desolvation for protein-ligand interactions (36-37) and for DNA triplex formation (38)

Comparison of the solvation free energies calculated with explicit waters and the continuum model shows similar trends but the actual numbers are significantly different, especially for the mutant. This comparison shows both the usefulness and limitation of the continuum solvent approach.

The proximity analysis results are given in Tables II and III for the wild type and the mutant, respectively and Table IV gives the differences between the two conformations for both the wild type and the mutant. The data is presented concatenated to residues and to the whole molecule.

Table III.
Proximity analysis results on Lys8-GnRH

	Conf.	$V_{\rm fs}$	$\langle K\rangle$	$\langle K\rangle/V_{\rm fs}$	$\langle BE\rangle$	$\langle BE\rangle/\langle K\rangle$	$\langle E_{\rm ww}\rangle$
PYR	Turn	852.0	23.79	0.84	-32.79	-1.38	-3.509
HIS	Turn	514.0	11.90	0.70	-26.06	-2.19	-3.476
TRP	Turn	701.1	15.14	0.65	-16.51	-1.09	-3.550
SER	Turn	270.1	5.90	0.66	-18.97	-3.22	-3.492
TYR	Turn	828.2	21.71	0.79	-27.44	-1.26	-3.435
GLY	Turn	192.4	4.16	0.65	-13.24	-3.19	-3.376
LEU	Turn	809.5	21.13	0.79	-22.16	-1.05	-3.487
LYS	Turn	576.8	14.98	0.78	-79.93	-5.34	-3.213
PRO	Turn	520.2	14.20	0.82	-32.76	-2.31	-3.504
GLY	Turn	219.1	4.69	0.64	-14.14	-3.02	-3.412
NH2	Turn	50.3	0.11	0.06	-0.28	-2.66	-3.384
GnRH	Turn	5534.	137.70	0.75	-284.28	-2.06	-3.450
PYR	Ext.	857.6	25.06	0.88	-32.21	-1.29	-3.332
HIS	Ext.	569.9	14.16	0.75	-23.54	-1.66	-3.490
TRP	Ext.	712.7	16.16	0.68	-15.18	-0.94	-3.546
SER	Ext.	376.9	10.22	0.82	-19.48	-1.91	-3.534
TYR	Ext.	742.6	19.81	0.80	-28.81	-1.45	-3.503
GLY	Ext.	275.4	7.15	0.78	-17.23	-2.41	-3.588
LEU	Ext.	586.4	14.19	0.73	-15.14	-1.07	-3.458
LYS	Ext.	636.9	17.18	0.81	-74.19	-4.32	-3.211
PRO	Ext.	521.2	13.98	0.81	-21.96	-1.57	-3.409
GLY	Ext.	348.7	9.21	0.79	-18.06	-1.96	-3.272
NH2	Ext.	51.4	0.10	0.06	-0.27	-2.59	-3.471
GnRH	Ext.	5680.	147.23	0.78	-266.07	-1.81	-3.428

Legend: The quantities are defined in Section II.2. Energies are in kcal/mol. The first shell density is given in g/ml.

The atoms on Fig. 1 are color coded by the water-water pair energies in the proximity regions of the various atoms. Atoms colored black are inaccesible to the solvent. The $E_{\rm ww}$ values should be compared to the corresponding value in the pure water run, -3.378 kcal/mol showing, that most residues have a structure making effect on the water (shown by colors green, yellow or red). The notable exceptions are the charged residues and the proline-9 of the mutant. Also, the structure-breaking atoms (colors cyan, blue or magenta) appear to cluster into relatively small regions. This indicates that structure breaking is a cooperative phenomenon and thus provides an explanation for the conformation dependence exhibited by some of the residues.

Table IV.

Proximity analysis difference (turn-extended) results on wild type and Lys8-GnRH

	$V_{\rm fs}$	$\langle K\rangle$	$\langle K\rangle/V_{\rm fs}$	$\langle BE\rangle$	$\langle BE\rangle/\langle K\rangle$	$\langle E_{\rm ww}\rangle$
PYR	-70.0	-4.58	-0.09	-1.29	-0.34	0.006
HIS	25.1	0.62	0.00	4.57	0.53	0.018
TRP	-102.6	-6.03	-0.17	6.18	-0.05	-0.020
SER	-171.0	-5.81	-0.12	-0.96	-1.52	-0.029
TYR	104.0	3.01	0.01	-1.18	0.14	0.002
GLY	-1.8	-0.28	-0.04	1.63	0.16	-0.047
LEU	79.3	1.32	-0.02	-2.03	-0.03	0.052
ARG	-11.6	-0.89	-0.04	-6.24	-0.80	-0.108
PRO	-56.5	-1.97	-0.04	4.06	0.09	-0.121
GLY	-215.7	-7.78	-0.32	13.17	-0.24	-0.228
NH2	-18.4	0.02	0.04	-0.11	-0.48	0.151
GnRH	-439.	-22.38	-0.07	17.79	-0.14	-0.031
PYR	-5.6	-1.27	-0.04	-0.58	-0.09	-0.178
HIS	-55.9	-2.26	-0.05	-2.52	-0.53	0.014
TRP	-11.6	-1.02	-0.03	-1.33	-0.15	-0.004
SER	-106.7	-4.33	-0.16	0.51	-1.31	0.042
TYR	85.5	1.90	-0.01	1.37	0.19	0.068
GLY	-83.0	-3.00	-0.13	3.99	-0.78	0.212
LEU	223.2	6.95	0.06	-7.02	0.02	-0.028
LYS	-60.1	-2.20	-0.03	-5.73	-1.02	-0.002
PRO	-1.0	0.22	0.01	-10.80	-0.74	-0.095
GLY	-129.6	-4.52	-0.15	3.91	-1.06	-0.140
NH2	-1.1	0.00	0.00	-0.01	-0.07	0.087
GnRH	-146.	-9.53	-0.03	-18.21	-0.26	-0.022

Legend: The quantities are defined in Section II.2. Energies are in kcal/mol. The first shell density is given in g/ml. It is clear from the analysis that the conformational free energy difference comes from many contributions of opposing directions and various sizes. The change due to the mutation is not a local effect of the mutated residue since for both molecules the turn conformation has both lower solute-solvent energy and lower near-neighbour solvent-solvent pair energy. The analysis shows that the turn conformation has reduced first solvation shell volume (especially the wild type) — this correlates with the reduction in the solute-solvent energy. However, the correlation is not uniform at the residue level, showing again the complexity of the solvation of GnRH.

Acknowledgement.

Fruitful discussions with Dr. Nina Pastor are gratefully acknowledged.

References.

1. S.C. Sealfon, H. Weinstein, and R.P. Millar, *Endocrine Reviews, 18,* 180, 1997).

2. F.A. Momany, *J. Amer. Chem. Soc., 98,* 2990 (1976).

3. F. Guarnieri, and S.R. Wilson, *J.Comput. Chem., 15,* 1302 (1994).

4. F. Guarnieri, H. Weinstein, *J. Amer. Chem. Soc., 118,* 5580-5589 (1996).

5. E.L. Baniak, J.E. Rivier, R.S. Struthers, A.T. Hagler, L.M. Gierasch, *PROTEINS: Structure, Function, and Genetics, 8,* 295 (1986).

6. M. Mezei, S. Swaminathan, and D.L. Beveridge, *J. Amer. Chem. Soc., 100,* 3255 (1978).

7. M. Mezei, and D.L. Beveridge, *Ann. Acad. Sci. N.Y., 482,* 1 (1986).

8. P.K. Mehrotra, and D.L. Beveridge, *J. Amer. Chem. Soc., 102* 4287 (1980).

9. N.A. Metropolis, A.W. Rosenbluth, M.N. Rosenbluth, A.H. Teller, and E. Teller, *J. Chem. Phys., 21,* 1087 (1953).

10. M. Rao, C.S. Pangali, and B.J. Berne, *Molec. Phys., 37,* 1779 (1979).

11. M. Mezei, *Mol. Simul., 5,* 405 (1991).

12. J.C. Owicki, in *Computer Modeling of Matter,* P.G. Lykos, Ed., American Chemical Society, Washington, D.C. (1978).

13. M. Mezei, *Mol. Simul., 1,* 169 (1988).

14. Brady, and M. Karplus, ala dipeptide error

15. A.J. McCammon, *Science, 238,* 486 (1987).

16. D.L. Beveridge, and F.M. DiCapua, *Annu. Rev. Biophys. Chem., 18,* 431 (1989).

17. M. Mezei, *Mol. Simul., 10,* 225 (1993).

18. T.P. Straatsma, and J.A. McCammon, *Annu. Rev. Phys. Chem., 43,* 407 (1992).

19. M. Mezei, in *Proton Transfer in Hydrogen-Bonded Systems*, T. Bountis, ed., Plenum, New York, (1992).

20. M. Mezei, *Mol. Simul., 2,* 201 (1989).

21. M. Mezei, *Molec. Phys., 67,* 1205 (1989), erratum to *47*, 1307 (1982).

22. M. Mezei, *J. Comput. Chem., 13,* 651 (1992) .

23. H. Resat, and M. Mezei, *J. Chem. Phys., 99,* 6052 (1993).

24. J.G. Kirkwood, In *Theory of Liquids*, B.J. Alder, Ed. Gordon and Breach. New York, NY (1968)

25. M.R. Mruzik, F.F. Abraham, D.E. Schreiber, and G.M. Pound, *J. Chem. Phys. 64,* 481 (1971).

26. W.C. Swope, H.C. Andersen, P.H. Berens, and K.R. Wilson, *J. Chem. Phys., 76,* 637 (1982).

27. M. Mezei, and D.L. Beveridge, *Methods in Enzymology, 127,* L. Packer, ed., 22-47 (1985).

28. G.F. Voronoi, *Z. Angew. Math. 134,* 198 (1908).

29. A. Ben-Naim, "Water and Aqueous Solutions," Plenum, New York (1974).

30. W. Fischer, and E. Koch, *Z. Kristall.*, *150,* 245 (1979).

31. M. Mezei, *Molec. Simul., 1,* 327 (1988).

32. W.L. Jorgensen, J Chandrashekar, J.D. Madura, R. Impey, and M.L. Klein, *J. Chem. Phys.*, *79,* 926 (1983).

33. R.B. Blackman, and J.W. Tuckey, The Measurement of Power Spectra, Dover (1958).

34. W.W. Wood, in *Physics of Simple Liquids.* Temperly, H.N.V., Rowlinson, F.S., and Rushbrooke, G.S., Eds., North-Holland (1968).

35. W.C. Still, A. Tempczyk, R.C. Hawley, and T. Hendrickson, *J. Amer. Chem. Soc., 112,* 6127 (1990).

36. C. Perez, M. Pastor, A.R. Ortiz, and F. Gago, *J. Med. Chem., 41,* 836, (1998)

37. A.R. Clarke, *Biochem. 37,* 2538, (1998)

38. K.G. Rajeev, V.R. Jadhav, and K.N. Ganesh, *Nucleic Acids Res., 25,* 4187 (1997)

39. H.J.C. Berendsen, J.P.M. Postma, W.F. Gunsteren, in *Molecular Dynamics and Protein Structure*, J. Hermans, ed., Polycrystal Book Service, Illinois, p 43 (1985).

40. R.W. Zwanzig, *J. Chem. Phys.*, *22,* 1420 (1954).

41. C.I. Bayly, and P.A. Kollman, *J. Amer. Chem. Soc.*, *116,* 697 (1994).

Date Received: October 26, 1998

Communicated by the Editor Ramaswamy H. Sarma